Electron-Phonon Interaction at the Si(111)-7 × 7 Surface

I. Barke, Fan Zheng, A. R. Konicek, R. C. Hatch, and F. J. Himpsel

Department of Physics, University of Wisconsin Madison, 1150 University Avenue, Madison, Wisconsin 53706, USA

(Received 14 December 2005; published 31 May 2006)

It is shown that electron-phonon interaction provides a natural explanation for the unusual band dispersion of the metallic surface states at the Si(111)-(7 × 7) surface. Angle-resolved photoemission reveals a discontinuity of the adatom band at a binding energy close to the dominant surface phonon mode at $\hbar\omega_0 = 70$ meV. This mode has been assigned to adatom vibrations by molecular dynamics calculations. A calculation of the spectral function for electron-phonon interaction with this well-defined Einstein mode matches the data. Two independent determinations of the electron-phonon coupling parameter from the band dispersion and from the temperature-dependent phonon broadening yield similar values of $\lambda = 1.09$ and $\lambda = 1.06$.

DOI: 10.1103/PhysRevLett.96.216801 PACS numbers: 73.20.−r, 73.61.Cw, 79.60.−i

Electron-phonon interaction determines a wide variety of phenomena, such as the pairing of electrons in superconductors, electrical conductivity of metals, and carrier scattering lengths in semiconductors. In recent years, it has become possible to measure the electron-phonon interaction by angle-resolved photoemission with high energy and momentum resolution [1]. As an energy band crosses the Fermi level E_F, there is a small region (one phonon energy $\hbar\omega_0$ wide) where the electron becomes dressed by phonons and acquires an extra effective mass. This leads to a break in the $E(k)$ band dispersion and a discontinuity of the group velocity at $E_F - \hbar\omega_0$. The ratio of the effective masses between a dressed and bare electron is related to the electron-phonon coupling parameter λ. Angle-resolved photoemission has made it possible to detect the electron-phonon coupling for specific bands at selected $\vec{k}$ points [for reviews, see [1]].

This method has been applied to metals, semimetals, and high-temperature superconductors, where the coupling to bosonic modes is the key to pairing. Surfaces exhibit a particularly strong electron-phonon interaction. By mapping two-dimensional energy bands at surfaces, one avoids perpendicular $\vec{k}$ broadening of the energy bands. In addition, there are well-defined surface phonon modes that are easier to identify than the continuum of bulk modes.

While there is plenty of evidence about electron-phonon interaction at metal surfaces from angle-resolved photoemission, there are no such results from semiconductors to our knowledge. Because of the gap, there are no sharp bands crossing the Fermi level. On the other hand, it has been recognized rather early that dangling-bond surface states have the potential for substantial electron-phonon interaction [2], and that such an interaction can influence surface reconstruction, which is ubiquitous on semiconductors. Contrary to most metal surfaces, the surface states on semiconductors contain significant charge and thus contribute substantially to the energetics of the surface. There are a few semiconductor surfaces with metallic surface states that offer the opportunity to observe the anticipated electron-phonon interaction. A classic example is the clean Si(111)-(7 × 7) surface with its odd number of electrons per unit cell [for an overview, see [3–8]]. The metallic electrons are located on the adatoms, whose broken bond states are partially filled. High-resolution photoemission is able to resolve a Fermi surface and to assign it to an electronlike adatom band [3]. In addition to its metallicity, the Si(111)-(7 × 7) surface exhibits a well-defined surface phonon mode at $\hbar\omega_0 = 70$ meV [9]. Calculations assign this mode to a vibration of an adatom against the atom underneath [10]. The close proximity of wave functions and phonon modes at the adatoms creates an environment for strong electron-phonon interaction between specific electron and phonon states.

Using high-resolution angle-resolved photoemission with variable temperature, we have been able to find evidence for electron-phonon interaction between the metallic adatom band and the adatom phonon mode. The data are compared quantitatively with a calculation of the spectral function for electron-phonon interaction with a discrete Einstein mode, and the interaction parameter λ is determined by a global fit to all photoemission spectra. A very similar λ is obtained independently from the temperature dependence of the linewidth. The results show that electron-phonon interaction is clearly a strong component in shaping the electronic structure of Si(111)-(7 × 7) near E_F and raise prospects for electron-phonon interaction studies at other semiconductor surfaces.

The band structure of the Si(111)-(7 × 7) surface in the vicinity of E_F is determined by a high-resolution Scienta 200U spectrometer with energy and angle multidetection. Synchrotron radiation with 34 eV photon energy and p polarization maximizes the cross section of the surface states. The setup and the sample preparation are similar to those described in [3], with the addition of a variable sample temperature (20–300 K). Particular care needs to be taken to determine the position of the Fermi level at low temperature, where a variety of semiconductor-specific

phenomena causes a shift and broadening of the Fermi edge, such as a photovoltage and a resistive potential gradient [for details, see [11]]. At low temperatures, the photovoltage saturates at the p- and n-type Schottky barrier, which is determined by the position of E_F in the gap [0.65 eV above the valence band maximum [12]]. The spatial variation of the photovoltage causes energy and momentum broadening. Our work covers a doping range from p-type 0.1 Ω cm to n-type 0.02 Ω cm. The results are independent of doping after correcting for the photovoltage shift by lining up the fully occupied rest-atom peak at $E_F - 0.8$ eV [for details see [11]]. The position of the Fermi level is determined at 300 K from the Fermi edges of the Mo sample clip and a Si(111)$\sqrt{3} \times \sqrt{3}$-Au surface [13] on a p-type substrate where the photovoltage is minimized. Because of residual photovoltage the Fermi cutoffs are shifted by $+5$ meV and -10 meV for p- and n-type Si(111)-(7×7) at 300 K, which is a measure of the accuracy in the absolute position of E_F.

Figure 1(a) shows the photoelectron intensity versus energy and momentum along the KΓK direction of the 7×7 Brillouin zone ($K_{7\times7} = 0.16$ Å^{-1}). High intensity is shown dark. The background from the rest-atom peak has been subtracted from each energy distribution curve (EDC) [see dashed lines in Figs. 1(d) and 1(e)]. The data consist of two energy regions of high intensity separated by a dip at -150 meV, which breaks up the adatom band into two parts [14]. The intensity maxima at -230 meV and -50 meV are located at $\Gamma_{7\times7}$ and near the Brillouin zone boundary, respectively. The change of the spectral weight is evident in the EDC shown in Figs. 1(d) and 1(e). On the left side, the Lorentzian tail of the rest-atom peak is visible. Taking into account momentum broadening, the peak at -230 meV is consistent with a band minimum at $E_0 = -280$ meV [3]. From momentum distribution curves close to E_F we obtain the Fermi wave vector $k_F = 0.15$ Å^{-1} and the group velocity $\nu_F = 3 \times 10^5$ m/s. The corresponding band filling is 1.8 electrons (90%). Along the MΓM direction the data are very similar, except for k_F being smaller by a factor $0.85 \approx \Gamma M/\Gamma K$ [see also Ref. [3]].

The electronic structure of Si(111)-(7×7) near E_F is characterized by adatom bands with an overall filling of 5 electrons. 12 adatoms donate 7 electrons from their broken bonds to fill the bond orbitals of $6 + 1$ rest atoms [3,6,8]. The additional 3.2 electrons need to be accommodated by a different band. A candidate is a lower-lying band associated with adatoms in the faulted half of the unit cell [7]. We observe a weak structure at -0.4 eV [shoulder in Fig. 1(e)] which could be the bottom of this band [for a detailed analysis see [11]]. Because of its large lifetime broadening, this band contributes only a featureless background.

The electron-phonon interaction is quantified by a calculation using the Einstein model for the Eliashberg function, which is appropriate for the dominant peak observed at $\hbar\omega_0 = 70$ meV in electron energy loss spectroscopy (EELS) [9]. For this model the complex self-energy Σ is easily obtained, and the momentum and energy dependent spectral function can be directly compared to the photo-

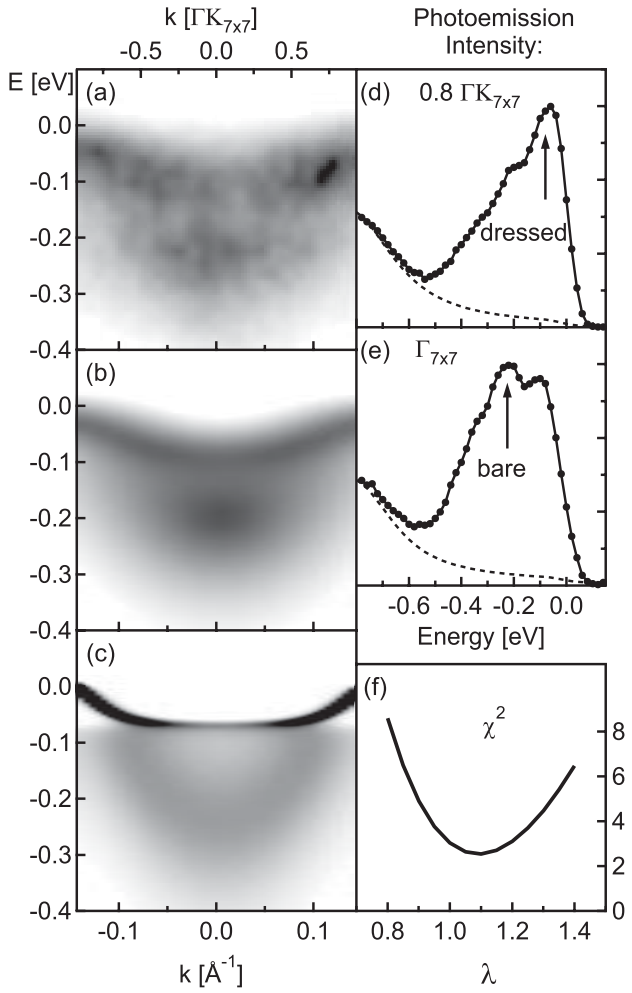

FIG. 1. Photoemission intensity vs energy E and momentum k for the metallic adatom bands of the Si(111)-(7×7) surface (top left). It is compared to the spectral function (bottom left), calculated for electron-phonon interaction with the 70 meV phonon observed by EELS [9] and assigned to adatom vibrations [10]. (a) Photoemission data at $T = 20$ K for a photon energy of 34 eV. High intensity is shown dark, and energies are relative to the Fermi level E_F. (b) Spectral function for an electron-phonon model with a single Einstein phonon mode at $\hbar\omega_0 = 70$ meV representing the observed surface phonon [9]. A Gaussian broadening has been applied in E and k. Best agreement with the data in (a) is obtained for an electron-phonon coupling constant $\lambda = 1.09$. (c) Spectral function (b) without broadening, to show the quasiparticle dispersion. (d) Energy distribution curve near k_F. The dressed band dominates the spectrum. (e) Energy distribution curve at the bottom of the band (Γ), where the bare band dominates. (f) Deviation χ^2 for a global fit to all photoemission spectra as a function of the electron-phonon coupling parameter λ.

emission data after accounting for the Fermi cutoff and the experimental broadening in E and k [1]. The bare electron dispersion $\varepsilon(k)$ is determined by the Fermi wave vector k_F and the bottom of the band $E_0 = -280$ meV within a parabolic approximation, yielding the effective mass $m^* = 0.31m_e$. It is consistent with previous studies in the direction MΓM [3]. Thus, the electron-phonon coupling λ and the convolution widths σ_k and σ_E are the only free parameters for fitting a total of 25 spectra simultaneously. The result is shown in Figs. 1(b) and 1(c), yielding a coupling constant $\lambda = 1.09$. Figure 1(f) shows the sum of squared differences χ^2 as a function of λ. The standard deviation calculated from the variance-covariance matrix is $\sigma_\lambda = 0.24$. The other parameters are $\sigma_k = 0.05$ Å^{-1} and $\sigma_E = 30$ meV.

The coupling constant λ has various effects on the calculated spectra. First, the ratio between the peak areas of the two peaks ("dressed" and "bare") in the EDC around $k = 0$ [see Fig. 1(e)] changes dramatically with λ. For $\lambda < 0.7$ the dressed band near E_F disappears in the tail of the bare band, while it dominates the spectra for $\lambda > 1.3$. The observed ratio can only be reproduced for $\lambda \approx 1$. Second, the width of the lower peak increases with λ. It is consistent with the data only for $\lambda \approx 1$. Finally, electron-phonon coupling causes an increasing line width at higher temperatures. Since this effect is not related to the low temperature data in Fig. 1, it provides an independent test for the validity of the electron-phonon coupling model.

The coupling parameter λ can be determined from the linear increase of the linewidth with T in the high-temperature limit $kT \gg \hbar\omega_{\max}$, where $\omega_{\max}$ is the highest phonon frequency: $\lambda = (2\pi)^{-1} d\Gamma/d(kT)$ [15]. At the lowest temperatures, the phonons are frozen out and Γ becomes independent of T. The linewidth is extracted from the temperature-dependent spectra in Fig. 2. These are taken near the boundary of the 7×7 Brillouin zone, where they can be approximated by a single Lorentzian. The energy scale has been referenced to the Fermi level of the metallic Si(111)$\sqrt{3} \times \sqrt{3}$-Au surface, with the rest-atom peak serving as fixed point to compensate photovoltage shifts at low temperature. In order to obtain the most reliable width Γ, only the energy regions most sensitive to Γ are selected for optimizing the fit [indicated by arrows in Fig. 2(a)]. A temperature-independent Gaussian convolution represents experimental broadening. The positions of the lines, and the ratio between a constant background and the secondary electron contribution below the rest-atom peak were treated as global fitting parameters with the same value for all temperatures. That leaves the Lorentzian widths $\Gamma(T)$ as the only free individual parameters in the fit, besides a normalization factor. The slope of the linear part of the resulting $\Gamma(T)$ curve in Fig. 2(b) ($T \geq 50$ K) yields the coupling constant. The result is $\lambda = 1.06$ for the adatoms, which independently confirms the value $\lambda = 1.09$ determined from the fit of the spectral function at

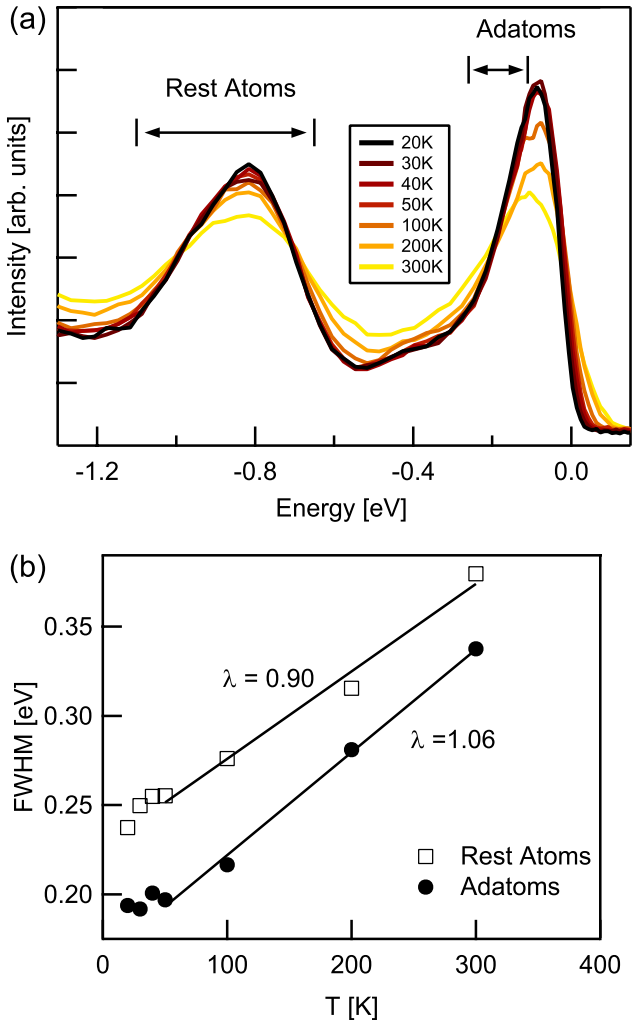

FIG. 2 (color online). Independent determination of the electron-phonon coupling constant λ for from the temperature-dependent width of the photoemission spectra, obtained for adatom and rest-atom bands. The value $\lambda = 1.06$ for the adatoms is close to $\lambda = 1.09$ from the spectral function (Fig. 1). (a) Temperature-dependent photoemission spectra for $k^{\parallel} = 0.13$ Å^{-1} along the $[11\bar{2}]$ azimuth (near $M_{7\times7}$). (b) Lorentzian peak widths Γ vs temperature for rest atoms and adatoms, obtained by fitting the two energy ranges marked in (a). The slope $d\Gamma/d(kT)$ of the linear region yields the electron-phonon coupling parameter λ.

$T = 20$ K. In addition, we obtain $\lambda = 0.9$ for the rest atoms, a second type of surface atoms with broken bonds which are associated with the peak at -800 meV in Fig. 2(a). Their phonon modes are different from those of the adatoms, though [10]. Since $T \leq 300$ K $< \hbar\omega_{\max}$ for all data presented here, the result represents a lower limit for λ. Corrections to this approximation are small for temperatures above $kT \approx \hbar\omega_{\max}/3$ [16].

Two additional, less accurate methods for determining λ serve as extra consistency checks. λ can be obtained from the width of the bare peak at low temperature, which is

caused by the lifetime broadening for phonon emission. For binding energies much larger than the phonon energy it is given by $\lambda \leq \Gamma/\pi\bar{E}_{\mathrm{ph}}$, where $\bar{E}_{\mathrm{ph}}$ is the average phonon energy [17]. The coupling parameter may be smaller due to other contributions to the overall line width. A fit of two peaks to the EDC at $k = 0$, one for the bare, the other for the dressed band, yields a Lorentzian width of $\Gamma = (230 \pm 40)$ meV for the lower peak. Applying the Einstein model again with $\bar{E}_{\mathrm{ph}} = \hbar\omega_0 = 70$ meV we end up with $\lambda \approx 1$, which is consistent with the more accurate determinations from the spectral function and the temperature broadening. Finally, we obtain $\lambda = 1.1$ from mass renormalization by comparing the group velocities at the Fermi level for the bare and dressed bands. For the dressed band, we take the Fermi velocity $\nu_F = 3 \times 10^5$ m/s from the momentum distribution curves, and for the bare band we obtain it from a parabolic fit to k_F and the bottom of the band E_0. The Fermi wave vector is common to both bands.

The strength of the electron-phonon interaction at the Si(111)-(7 × 7) surface is in the range of λ reported for metal surfaces [$\lambda \approx 0.5$–1.4, see [1] for a tabulation]. There is an important difference from metals, though. For the Si(111)-(7 × 7) surface, a large fraction of the band (40% of the density of states) is located within the dressed region that lies within $\pm\hbar\omega_0$ around E_F. This fraction is negligible in most metals where the band width is typically 2 orders of magnitude larger than the phonon energy.

In summary, we are able to make a strong case for electron-phonon interaction shaping the band dispersion near the Fermi level at the Si(111)-(7 × 7) surface, combining temperature-dependent, angle-resolved photoemission data with previous electron energy loss results [9] and molecular dynamics calculations of surface phonons [10]. The spectral function is calculated with most of the input parameters constrained by the experimental data about the phonon mode, the bottom of the band, and the Fermi wave vector. The remaining fit parameter is the electron-phonon coupling constant, which comes out to be $\lambda = 1.09$. As a cross-check we determine λ independently from the temperature-dependent width of the photoemission spectra and obtain a very similar value $\lambda = 1.06$. Two further estimates confirm that $\lambda \approx 1$.

The results break new ground by addressing electron-phonon interaction on semiconductor surfaces. A well-defined phonon mode interacts with a specific electronic state, both located on the adatoms of the Si(111)-(7 × 7) surface. This finding validates the early prediction [2] that semiconductor surfaces with their localized broken bonds are excellent candidates for studying the coupling with a specific phonon mode. Many other semiconductor surfaces are characterized by special surface atoms with broken bond orbitals and distinct vibrational modes associated with the altered bond geometry. The Si(111)-(7 × 7) surface itself combines strong electron-phonon interaction with a bandwidth more than twice as large as ground state calculations. Both make this surface a highly interesting system for many body physics.

The experimental setup at the Synchrotron Radiation Center (SRC) and the help of S. Janowski, H. Höchst, M. Bissen, M. Fisher, and S. Gorovikow are gratefully acknowledged. F. J. H. enjoyed helpful discussions with D. Fick on the Si(111)-(7 × 7) surface. The work was supported by the NSF under Grants No. DMR-0240937 and No. DMR-0084402 (SRC). I. B. was supported by the German Academic Exchange Service (DAAD).

[1] E. W. Plummer *et al.*, Prog. Surf. Sci. **74**, 251 (2003); C. Kirkegaard, T. K. Kim, and Ph. Hofmann, New J. Phys. **7**, 99 (2005).
[2] C. Tejedor, F. Flores, and E. Louis, J. Phys. C **19**, 543 (1986).
[3] R. Losio, K. N. Altmann, and F. J. Himpsel, Phys. Rev. B **61**, 10 845 (2000).
[4] J. M. Layet *et al.*, Phys. Rev. B **30**, R7355 (1984).
[5] R. I. G. Uhrberg, T. Kaurila, and Y.-C. Chao, Phys. Rev. B **58**, R1730 (1998).
[6] R. Schillinger *et al.*, Phys. Rev. B **72**, 115314 (2005).
[7] R. D. Meade and D. Vanderbilt, Phys. Rev. B **40**, 3905 (1989).
[8] J. Ortega, F. Flores, and A. L. Yeyati, Phys. Rev. B **58**, 4584 (1998); F. Flores, A. L. Yeyati, and J. Ortega, Surf. Rev. Lett. **4**, 281 (1997).
[9] W. Daum, H. Ibach, and J. E. Müller, Phys. Rev. Lett. **59**, 1593 (1987).
[10] J. Kim *et al.*, Phys. Rev. B **52**, 14 709 (1995).
[11] I. Barke *et al.* (to be published).
[12] F. J. Himpsel, G. Hollinger, and R. A. Pollak, Phys. Rev. B **28**, 7014 (1983); 0.65 eV is an updated value.
[13] K. N. Altmann *et al.*, Phys. Rev. B **64**, 035406 (2001) and references therein.
[14] As an alternative to the electron-phonon interaction we have considered two-band models, where the intensity dip corresponds to a band gap. Local density theory [8] produces a pair of flat hole bands that cross E_F. These are separated from a lower-lying electron band by a small gap. However, the dispersion in Fig. 1(a) shows that the band is electronlike at E_F, not holelike. An interaction with a localized state has been proposed for creating a minigap on Si(111)$\sqrt{3} \times \sqrt{3}$-Ag [see J. N. Crain *et al.*, Phys. Rev. B **72**, 045312 (2005)] and C. Liu *et al.*, Phys. Rev. Lett. **96**, 036803 (2006)). As a third option one could consider a Hubbard gap [see [6,8,11] and references therein].
[15] G. Grimvall, in *The Electron-Phonon Interaction in Metals, Selected Topics in Solid State Physics*, edited by E. Wohlfarth (North-Holland, Amsterdam, 1981).
[16] B. A. McDougall, T. Balasubramanian, and E. Jensen, Phys. Rev. B **51**, R13891 (1995); V. N. Kostur and B. Mitrovic, Phys. Rev. B **48**, 16 388 (1993); T. Balasubramanian, P.-A. Glans, and L. I. Johansson, Phys. Rev. B **61**, 12 709 (2000).
[17] E. Rotenberg, J. Schaefer, and S. D. Kevan, Phys. Rev. Lett. **84**, 2925 (2000); S.-J. Tang *et al.*, Phys. Status Solidi B **241**, 2345 (2004).